

Charge injection in molecular wires grafted on metallic surfaces: electron-lattice interaction

H. Ness^{1,a} and A.J. Fisher^{2,b}

¹ CEA-Saclay, DSM/DRECAM/SPCSI, bâtiment 462, 91191 Gif-sur-Yvette, France

² Department of Physics and Astronomy, University College London, Gower Street, London WC1E 6BT, UK

Received 10 September 2002

Published online 3 July 2003 – © EDP Sciences, Società Italiana di Fisica, Springer-Verlag 2003

Abstract. We study the injection of single charge carrier in one-dimensional molecular wires in the presence of coherent electron-lattice coupling. We show that charge injection at the molecule/metal interface induces lattice distortions in the molecule itself reflecting the formation of polaron-like defect. The behaviour of the charge density of the injected carrier and the mean position of the carrier depend strongly on the value of the injection energy relative to the band edges of the molecular wires.

PACS. 73.63.-b Electronic transport in mesoscopic and nanoscale materials and structures – 73.40.Gk Tunneling – 73.61.Ph Polymers; organic compounds

1 Introduction

With the recent progress in nanoscale fabrication techniques, the measurement of the electronic transport properties of individual examples of quasi one-dimensional molecular systems is now possible [1–3]. Such quasi one-dimensional systems may be expected to exhibit enhanced effects of correlations during electron injection and transport. For example, the electron-lattice coupling can lead to the Peierls transition [4], which opens a gap at the Fermi energy and renders one-dimensional metallic systems semiconducting.

In recent papers we addressed this problem, in the context of molecular wires [5,6]; by considering finite length poly-acetylene chains described by a fully quantum version of the Su–Schrieffer–Heeger (SSH) model [7]. The Peierls transition manifests itself in an alternation of single and double bonds (*i.e.*, *dimerisation*) along the molecule, and therefore the presence of a substantial gap between the Highest Occupied Molecular Orbital (HOMO) and the Lowest Unoccupied Molecular Orbital (LUMO). Bulk electron transport is dominated by mobile intrinsic defects formed when charge carriers are injected into this dimerised structure. The most important defects are polarons (local reduction in the dimerisation around an injected charge) and charged solitons (topological defects in the bond length alternation). In order to understand transport through these systems, we have developed a theory of coherent transport that accounts for polaron and soliton formation [5,6,8].

In this paper, we consider the carrier injection from a single electrode into the molecule. In this context, charge

injection can be seen as the first event of a sequence of steps in the overall process of transport through a molecule or a molecular film. This first event might be followed by other different events inside the molecule (for example, electron/hole recombination, relaxation of the geometry of the molecule, etc.); which are considered to be uncorrelated. However, we consider the injection process to be a single coherent event. It is complicated by the presence of the relaxation of the geometry of the molecule due to the interaction between the injected charge and the molecular lattice. This electron-phonon (*e-ph*) coupling produces the relaxation in a similar way to the polaron formation we observed in our previous studies of electron transport in molecular wires [5,8].

In transport measurements it is only the combined result of all the processes [9] that would be observed, and the contribution from the injection step could only be isolated by looking at the dependence on external parameters such as the temperature or the chemical potential of the injected carriers, which could be controlled by an external gate or by chemical means.

2 The model

We are interested in modeling the coherent injection of an electron inside a molecular wire, where the electron also interacts with extended vibrational modes of the molecule. The Hamiltonian for the molecule is

$$H = \sum_n \epsilon_n c_n^\dagger c_n + \sum_\lambda \hbar\omega_\lambda a_\lambda^\dagger a_\lambda + \sum_{\lambda,n,m} \gamma_{\lambda nm} (a_\lambda^\dagger + a_\lambda) c_n^\dagger c_m, \quad (1)$$

^a e-mail: ness@drecom.saclay.cea.fr

^b e-mail: Andrew.Fisher@ucl.ac.uk

where c_n^\dagger (c_n) creates (annihilates) an electron in the n th electronic state with energy ϵ_n . These states are taken to be the one-electron eigenstates of the reference system; in the case of conjugated polymers, they correspond to π -electron states delocalized along the molecule. The electrons interact with the vibrational modes λ of the molecule (a_λ^\dagger creates a quantum of energy $\hbar\omega_\lambda$ in the mode λ) via the e -ph matrix elements $\gamma_{\lambda nm}$. The parameters ϵ_n , ω_λ and $\gamma_{\lambda nm}$ are obtained from the ground state of the isolated neutral molecule containing N monomers. This neutral molecule is described by the well-known SSH model [7, 10]. The molecule eigenmodes of vibration and their frequencies ω_λ are calculated within the harmonic approximation for the lattice distortions [11].

The molecule is connected to one metallic electrode by one end (the left end for example). Then its discrete electronic spectrum is coupled to the continuum of states of the electrode. There is no net current passing through the molecule, however an electronic wave function can penetrate from the metal into the molecular wire. For simplicity, we use a tight-binding model for the one-dimensional semi-infinite metallic electrode (on-site energy ϵ_L , intersite hopping matrix element β_L and v_L the hopping matrix element between the molecule end and the electrode).

In order to study the effect of charge injection, we use the same stationary-state inelastic scattering technique that we developed to study transport through molecular wires [5, 8]. The scattering states $|\Psi\rangle$ for a single injected electron are expanded (in the molecule) onto the eigenstates $|n, \{n_\lambda\}\rangle = c_n^\dagger \prod_\lambda (a_\lambda^\dagger)^{n_\lambda} / (\sqrt{n_\lambda!}) |GS\rangle$ of the non-interacting e -ph system, where n_λ is the occupation of the vibrational mode λ and $|GS\rangle$ the ground state of the neutral molecule. The states $|n, \{n_\lambda\}\rangle$ correspond to adding a single charge to this reference state, and adding a definite number of quanta to each vibrational mode λ . Then the problem is transformed into a single-electron problem with many scattering channels [8, 12]. Each of the possible scattering process between the injected charge and the vibrational modes is associated with a different channel. For a given energy E , the amplitude for each of these processes is found by solving the following complex linear system $|\Psi(E)\rangle = G(E)|s(E)\rangle$ in the molecule Hilbert subspace¹. The Green's function $G(E)$ defined in the molecule subspace is given by $G(E) = [E - H - \Sigma_L(E)]^{-1}$ where H is defined in equation (1) and $\Sigma_L(E)$ is the energy-dependent complex potential arising from embedding the molecule's spectrum into the electrode continuum of electronic states. $|s(E)\rangle$ is the source term state for electron injection at energy ϵ_{in} from the left electrode. For an initial phonon configuration given by the occupation numbers $\{m_\lambda\}$, we have $E = \epsilon_{in} + \sum_\lambda m_\lambda \hbar\omega_\lambda$ because the system conserves its total energy. In this paper, we consider the limit of low temperatures: the phonons are initially in the ground state ($m_\lambda = 0$ for all λ) and therefore $\epsilon_{in} = E$. Once the linear system $|\Psi\rangle = G(E)|s\rangle$ is solved, all expectation values can be calculated from the known scattering state $|\Psi\rangle$. In the next section, we present results for the

Table 1. Energy (in eV) of the LUMO level and of the polaron resonance for different molecule lengths N .

N	20	40	60	80	100	140
E_{LUMO}	0.957	0.644	0.547	0.504	0.481	0.459
$E_{\text{pol res}}$	0.889	0.559	0.459	0.423	0.388	0.372

total electron density $|\langle j|\Psi(E)\rangle|^2$ at site j and the mean electron position $\langle x \rangle$ defined by $\langle x(E) \rangle = \sum_j j |\langle j|\Psi(E)\rangle|^2$.

3 Results and discussion

In principle, the energy of the injected electron depends on the position of the Fermi level of the metallic electrode relative to the electronic states of the molecular wire. The problem of the electrostatics and charge density should be solved self-consistently to determine such energy level alignment, including possible charge transfers between the metal and the molecule [13]. However for the model used here, the energy E of the injected electron is considered as being variable. This permits us to explore the different possible physical conditions.

In this section, we present results for molecules made of an even number N of monomers. Within the model, a neutral molecule of length N contains $N/2$ doubly-occupied π -electron states and has a HOMO-LUMO gap ranging from ≈ 1 to 2 eV. Owing to charge conjugation symmetry, the energy reference $E = 0$ is exactly at mid-gap in between the HOMO and LUMO levels for each molecule. The gap can be easily deduced from the value of E_{LUMO} given in Table 1. The injected electron is coupled to the $N_{\text{ph}} = 4$ longest wavelength optic modes λ of the molecule and we restrict the maximum number of excitations in each mode to $n_{\text{occ}}^{\text{max}} = 2$. We have checked that the results obtained for such a truncated phonon subspace are fairly well converged. Furthermore the exact values of the results depend on the other parameters (v_L and β_L). The influence of the band-width ($4\beta_L$) of the electrode is relatively small as far as this band-width is of the same order of magnitude (or much larger) than the electronic spectrum of the molecule. The influence of metal/molecule coupling matrix element v_L is more subtle. For example, the electron density at the left side of the wire $|\langle j = 1|\Psi\rangle|^2$ is proportional to v_L^2 . However, we have checked that the qualitative physics of charge injection presented below remains the same for different values of these parameters.

For an initial energy E at mid-gap, the typical behaviour of the electron density $|\langle j|\Psi(E)\rangle|^2$ at site j is shown in Figure 1 for the molecule length $N = 140$. The overall shape of the electron density is characteristic of an exponentially decaying wave function inside a tunneling barrier. The small oscillations from site to site in the electron density reflect the shape of the molecular one-electron states $|n\rangle$ used to construct $|\Psi\rangle$. However to emphasize the different effects on the global shape of the electron density, we have calculated a smoother density by averaging out these oscillations (left and right panels in Fig. 1).

¹ The phonon subspace is truncated to contain up to a maximum number of phonon excitations $n_{\text{occ}}^{\text{max}}$ in each mode λ .

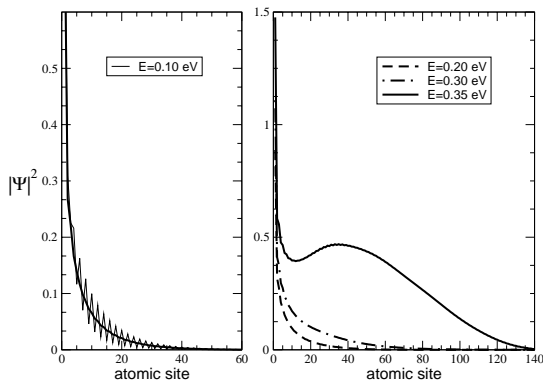


Fig. 1. Electron density $|\langle j|\Psi(E)\rangle|^2$ on site j for different injection energies E inside the HOMO-LUMO gap of the molecule (length $N = 140$). The electron density oscillates from site to site (left panel), a smoother density is obtained by averaging out the oscillations (left and right panels). For energies deep inside the gap, the electron density decays exponentially from the metal/molecule interface ($j = 0$) into the molecule itself as expected for an electron inside a tunneling barrier.

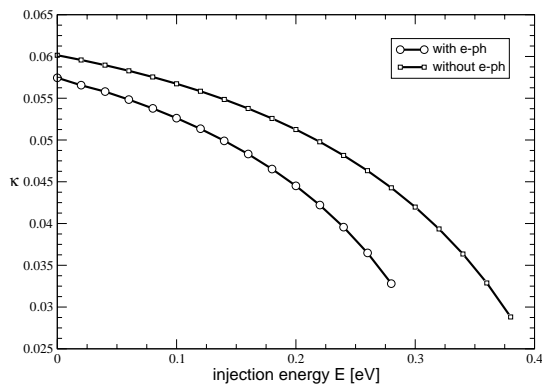


Fig. 2. Decay rate $\kappa(E)$ of the electron density (molecule length $N = 140$) for injection energies deep inside the gap. $\kappa(E)$ is obtained from the best fit of $|\langle j|\Psi(E)\rangle|^2$ onto $\exp(-2\kappa(E)x_j)$. In the presence of e -ph coupling, the decay rate κ is smaller reflecting a lower effective barrier height.

For energies around mid-gap (for example $0 \leq E \leq 0.20$ and 0.30 eV in the case of a $N = 100$ and $N = 140$ chain length respectively), the decay rate $\kappa(E)$ of the electron density follows roughly the usual square-root law of a tunneling electron inside a square tunnel barrier (Fig. 2). The electron density decays faster for energy E well below the “barrier height”. However, this behaviour occurs only for injection deep inside the gap of the molecule. Because of the e -ph coupling, the electron density behaves differently for higher energies as shown in Figure 3. For injection energies E increasing towards the valence band edge E_{LUMO} , the electron density no longer behaves like a purely decaying function in the molecule itself (Figs. 1 and 3). The electron density takes the shape of a resonance that is mostly symmetric and located at the center of the molecule. This behaviour is maximized for injection at the polaron resonance energy $E_{\text{pol res}}$ that we observed

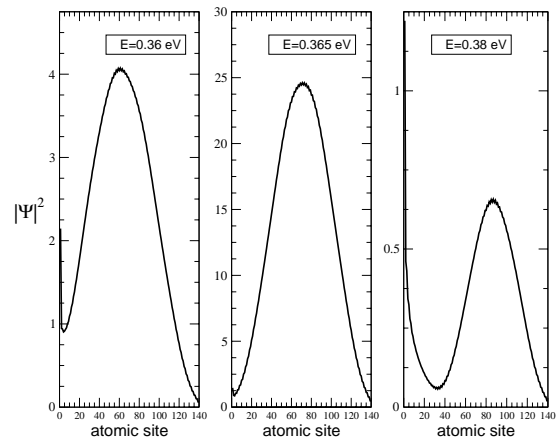


Fig. 3. Electron density in a molecule of length $N = 140$ for energies E increasing towards the band edge E_{LUMO} . Around the polaron resonance ≈ 0.365 eV, the electron density is more symmetric and localized at the centre of the molecule, in contrast to the results obtained for injection deep inside the gap.

in the electron transmission curves in our study on transport in the molecular wires [5,6,8]. The values of the polaron resonance $E_{\text{pol res}}$ are given in Table 1 for different molecule lengths.

For injection energies above the polaron resonance but still below E_{LUMO} , the electron density displays two features: an exponential decay from the metal/molecule interface into the molecule and a peak in the middle of the molecule indicating that a part of the electron density is located around the center of the molecule (Fig. 3).

Now we discuss the effects of the e -ph coupling. Figure 2 shows that the decay rate $\kappa(E)$ varies roughly as expected for an electron wave function inside a square tunnel barrier with a barrier height given by the electronic level just above the gap E_{LUMO} (shifted by the real part of Σ_L). However $\kappa(E)$ is reduced in the presence of e -ph coupling, invoking an apparent reduction of the effective barrier height. This is not surprising because the injected electron (even for injection deep inside the gap) induces distortions of the molecule lattice. We have already shown that such distortions correspond to the formation of a virtual polaron [5,8]. The polaron formation is also associated with a relaxation energy that shifts the electronic energy levels of the system. Consider the simple case of one electron coupled to a single phonon mode (frequency ω and e -ph coupling constant γ) on a single site, the corresponding relaxation energy is $-\gamma^2/\hbar\omega$ and the molecular electronic levels are shifted accordingly, in the limit of weak coupling (v_L) to the electrode. In the case of intermediate coupling to the electrode, one might expect to see an intermediate shift of the electronic levels. In our model Hamiltonian (Eq. (1)), the injected electron is coupled to different phonon modes *via* the coupling matrix elements $\gamma_{\lambda nm}$. It is not straightforward to obtain a simple expression for the corresponding relaxation energy because the e -ph coupling term is not diagonal in the electron subspace; however, one observes the same trends: the relaxation shifts the electronic levels and one obtains an

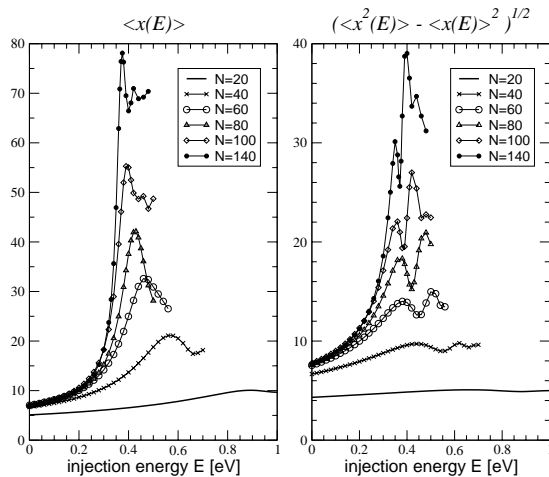


Fig. 4. Mean position $\langle x \rangle$ and mean width $(\langle x^2 \rangle - \langle x \rangle^2)^{1/2}$ of the injected electron in molecules of different lengths N .

effective reduction of the apparent tunneling barrier (see Fig. 2).

The variations of the electron density and the effects of the e -ph coupling are also reflected in the mean position $\langle x(E) \rangle$ of the injected electron defined previously. We also calculate the second moment $\langle x^2(E) \rangle$ of the electron position and determine a corresponding mean width $\sqrt{\langle x^2(E) \rangle - \langle x(E) \rangle^2}$. Figure 4 shows the evolution of the mean position and mean width *versus* the injection energy E for different molecule lengths. For injection deep inside the gap, the electron penetration is weak (especially for short molecules) and most of the electron density is located at the end of the molecule connected to the electrode. As expected from the variation of the electron density, the electron penetration first increases slowly for increasing E values. Such a behaviour is also obtained by calculating $\langle x \rangle$ and $\langle x^2 \rangle$ from a normalized wave function $\phi(x) \propto \exp(-\kappa x)$ using the decay rate $\kappa(E)$ given in Figure 2. However, for injection energy approaching the polaron resonance, the mean position $\langle x \rangle$ increases rapidly. At the resonance the electron is located around the middle of the molecular chain. The corresponding wave function and electron density seems to be more localized as reflected by the decrease in the mean width at the polaron resonance energies. Finally, Figure 5 illustrates once more the shift of the molecular levels due to the e -ph coupling. Without e -ph coupling, the maximum value of $\langle x \rangle$ (roughly the middle of the molecule) occurs for an injection in resonance with E_{LUMO} , while in the presence of e -ph coupling, this maximum occurs for an injection energy lowered by the corresponding relaxation of the molecular lattice.

4 Conclusion

We studied coherent charge injection in molecular wires chemisorbed by one end on a model metallic surface. We

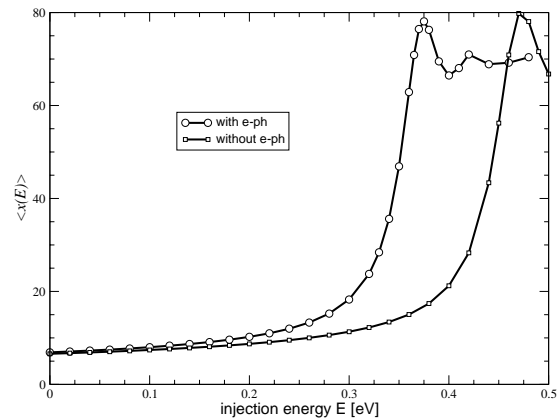


Fig. 5. Mean position $\langle x \rangle$ of the injected electron in the presence and in the absence of e -ph coupling.

studied electron wave function penetration from the metal into the molecule in presence of electron-vibration coupling inside the molecule. The electron density and mean electron position have been calculated for a wide range of electron injection energy and for different molecule lengths. The electron-vibration coupling induces distortions of the molecule lattice and leads to polaron formation. For injection deep inside the HOMO-LUMO gap of the molecule, electron penetration is mostly located at the metal/molecule interface. Only at and around the polaron resonance energy, the electron becomes more localized in the middle of the molecule. We also evaluate energy-dependent decay rate $\kappa(E)$ for the electron density. The dependence of κ *versus* E closely reassembles complex-band structure calculations from which the energy-dependent effective mass can be deduced [14].

References

1. Z.J. Donhauser *et al.*, Science **292**, 2303 (2001); V.J. Langlais *et al.*, Phys. Rev. Lett. **83**, 2809 (1999)
2. J. Reichert *et al.*, Phys. Rev. Lett. **88**, 176804 (2002); C. Kergueris *et al.*, Phys. Rev. B **59**, 12505 (1999); M.A. Reed *et al.*, Science **278**, 252 (1997)
3. N.B. Zhitenev *et al.*, Phys. Rev. Lett. **88**, 226801 (2002)
4. R.E. Peierls, *Quantum Theory of Solids* (Clarendon Press, Oxford, 1955), p. 110
5. H. Ness, A.J. Fisher, Phys. Rev. Lett. **83**, 452 (1999)
6. H. Ness, A.J. Fisher, Europhys. Lett. **57**, 885 (2002)
7. A.J. Heeger *et al.*, Rev. Mod. Phys. **60**, 781 (1988)
8. H. Ness *et al.*, Phys. Rev. B **62**, 125422 (2001)
9. A.M. Stoneham *et al.*, J. Phys. Cond. Matt. **14**, 9877 (2002)
10. W.P. Su *et al.*, Phys. Rev. B **28**, 1138 (1983); **22**, 2099 (1980); Phys. Rev. Lett. **42**, 1698 (1979)
11. K.A. Chao, Y. Wang, J. Phys. C **18**, L1127 (1985)
12. J. Bonča, S.A. Trugman, Phys. Rev. Lett. **75**, 2566 (1995)
13. M. Brandbyge *et al.*, Phys. Rev. B **65**, 165401 (2002)
14. C. Joachim, M. Magoga, Chem. Phys. **281**, 347 (2002)